The Role of S4 Charges in Voltage-dependent and Voltage-independent KCNQ1 Potassium Channel Complexes

Gianina Panaghie and Geoffrey W. Abbott

Greenberg Division of Cardiology, Department of Medicine and Department of Pharmacology, Cornell University, Weill Medical College, New York, NY 10021

Voltage-gated potassium (Kv) channels extend their functional repertoire by coassembling with MinK-related peptides (MiRPs). MinK slows the activation of channels formed with KCNQ1 α subunits to generate the voltage-dependent I_{Ks} channel in human heart; MiRP1 and MiRP2 remove the voltage dependence of KCNQ1 to generate potassium "leak" currents in gastrointestinal epithelia. Other Kv α subunits interact with MiRP1 and MiRP2 but without loss of voltage dependence; the mechanism for this disparity is unknown. Here, sequence alignments revealed that the voltage-sensing S4 domain of KCNQ1 bears lower net charge (+3) than that of any other eukaryotic voltage-gated ion channel. We therefore examined the role of KCNQ1 S4 charges in channel activation using alanine-scanning mutagenesis and two-electrode voltage clamp. Alanine replacement of R231, at the N-terminal side of S4, produced constitutive activation in homomeric KCNQ1 channels, a phenomenon not observed with previous single amino acid substitutions in S4 of other channels. Homomeric KCNQ4 channels were also made constitutively active by mutagenesis to mimic the S4 charge balance of R231A-KCNQ1. Loss of single S4 charges at positions R231 or R237 produced constitutively active MinK-KCNQ1 channels and increased the constitutively active component of MiRP2-KCNQ1 currents. Charge addition to the CO_2H-terminal half of S4 eliminated constitutive activation in MiRP2-KCNQ1 channels, whereas removal of homologous charges from KCNQ4 S4 produced constitutively active MiRP2-KCNQ4 channels. The results demonstrate that the unique S4 charge paucity of KCNQ1 facilitates its unique conversion to a leak channel by ancillary subunits such as MiRP2.

The Journal of General Physiology

INTRODUCTION

Voltage-gated ion channels mediate cellular electrical excitability and are thus essential for the action potentials of neurons, myocytes, and all other excitable cells. Voltage-gated sodium and calcium channels permit influx of their respective ions once the threshold voltage for their activation is attained. This influx of positive ions depolarizes the cell further, activating voltage-gated potassium (Kv) channels to allow efflux of K^+ ions, repolarizing the cell, and ending the action potential. All voltage-gated cation channels contain four voltage-sensing S4 domains (membrane-spanning α helices bearing basic residues) that confer voltage sensitivity. Upon cellular depolarization, S4 undergoes a conformational and/or positional change to the "on" position, which is communicated to the channel gate, opening the channel. The exact nature of the movement that S4 undergoes when switching from the "off" to the "on" position is a matter of intense debate, with some arguing for a comprehensive shift from the intracellular to the extracellular side of the plasma membrane, while others contend the conformational shift is far more subtle (Jiang et al., 2003; Starace and Bezanilla, 2004).

The KCNQ subfamily of Kv channel α subunits contains five known members, KCNQ1–5. While KCNQ2–5 are neuronally expressed and contribute to the M-current, KCNQ1 is expressed in the heart, gastrointestinal epithelia, and inner ear, but not the brain (Wang et al., 1998; Kubisch et al., 1999; Jentsch, 2000; Schroeder et al., 2000a; Jensen et al., 2005). MiRPs (MinK-related peptides), encoded by *KCNE* genes, are single transmembrane domain ancillary subunits that coassemble with a wide array of voltage-gated potassium (Kv) channels and hyperpolarization-activated, cation-nonselective (HCN) channels to alter their gating, conductance, regulation, and pharmacology (Takumi et al., 1988; Barhanin et al., 1996; Sanguinetti et al., 1996; Sesti and Goldstein, 1998; Abbott et al., 1999; Schroeder et al., 2000b; Tinel et al., 2000a,b; Abbott et al., 2001; Yu et al., 2001; Zhang et al., 2001; Lewis et al., 2004). KCNQ1 is unique among voltage-gated ion channels in that it can be converted to a voltage-independent, constitutively active, "leak" channel by association with ancillary subunits (MiRP1 and MiRP2) (Wang et al., 1998; Kubisch et al., 1999; Jentsch, 2000; Schroeder et al., 2000b). Indeed, even other KCNQ subfamily α subunits reportedly interact with MiRPs but do not become leak channels: KCNQ2/3 with MiRP1 and KCNQ4 with MiRP2 (Schroeder et al., 2000b; Tinel et al., 2000b).

Correspondence to Geoffrey W. Abbott: gwa2001@med.cornell.edu

Abbreviations used in this paper: HCN, hyperpolarization-activated, cation-nonselective; Kv, voltage-gated potassium; MiRP, MinK-related peptide; TEVC, two-electrode voltage clamp.

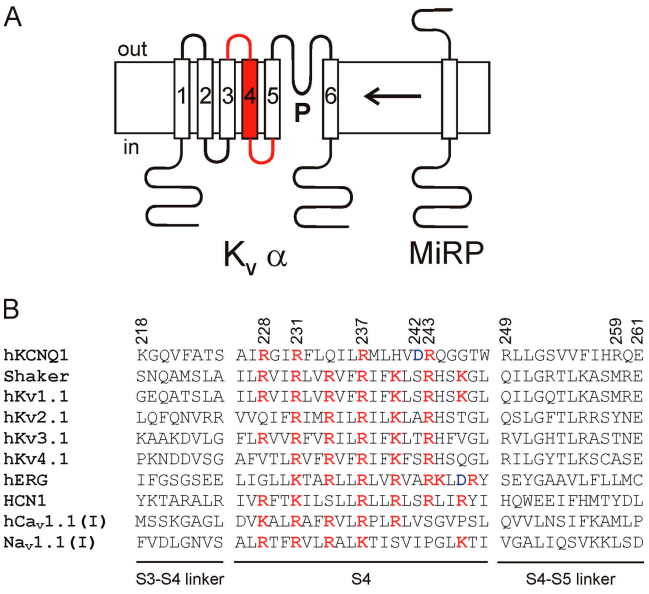

Figure 1. KCNQ1 topology and voltage sensor sequence. (A) The 6 transmembrane (TM) domain topology of Kv α subunits (left) and the 1 TM domain topology of *KCNE*—encoded ancillary subunits (MiRPs) (right). The S3–S4 linker, S4 domain, and S4–S5 linker are highlighted in red. (B) Sequence alignment for S3–S4 linker, S4, and S4–S5 linker in human K_v, HCN, Ca_v, and Na_v channels. S4 residues are colored: red, positive charges; blue, negative charges. The positions of KCNQ1 charged residues mutated to alanine in this study are indicated at the top.

This unique loss of voltage dependence is proposed to be crucial to the role of KCNQ1 in providing a K^+ ion leak conductance in the colon by association with MiRP2 (Schroeder et al., 2000b) and stomach with MiRP1 (Tinel et al., 2000a; Grahammer et al., 2001; Heitzmann et al., 2004; Roepke et al., 2006), in contrast to generating the voltage-dependent, slowly activating I_{Ks} repolarization current in the heart and inner ear with MinK, the founding member of the MiRP family (Barhanin et al., 1996; Sanguinetti et al., 1996; Warth and Barhanin, 2002). The propensity of KCNQ1 for conversion to leak mode by MiRP1 and MiRP2 poses several questions, three of which we address here: how can a channel with a voltage sensor lose voltage dependence; is the KCNQ1 activation gate uncoupled from S4 in leak channels; and why do MiRP1 and MiRP2 not convert any of their many other potassium channel partners to leak channels?

MiRPs exhibit promiscuity of interaction; each can associate with a number of different α subunit partners (McCrossan and Abbott, 2004). Furthermore, each MiRP exerts a range of functional effects depending upon the α subunit, thus α subunit sequence differences must be an important determinant of functional outcome. Previous studies have identified MiRP sequence motifs important in determining specific gating effects (Melman et al., 2002), but α subunit sequence motifs determining α subunit–specific gating effects have not previously been determined. Here, the results of alanine-scanning mutagenesis in KCNQ1 and reciprocal mutagenesis between KCNQ1 and KCNQ4 demonstrate that the charge paucity of the CO_2H half of KCNQ1 S4 underlies its susceptibility to conversion to leak mode, distinguishing it from its neuronal KCNQ relatives and, indeed, all other voltage-gated ion channels.

MATERIALS AND METHODS

Molecular Biology

Human KCNQ1 and KCNQ4 mutants were constructed using the QuickChange Multi Site-Directed Mutagenesis Kit (Stratagene). Mutant KCNQ1 and KCNQ4 genes were sequenced in their entirety to confirm appropriate mutations and check for inadvertent mutations and then subcloned back into oocyte expression vectors: (pYY1, KCNQ1; pTLN, KCNQ4). Wild-type human MinK and MiRP2 were cloned into pRAT. cRNA transcripts were produced from Not I–linearized (or Hpa I for KCNQ4) DNA templates using the T3 (KCNQ1), SP6 (KCNQ4), and T7 (MiRPs) mMessage mMachine kits (Ambion). cRNA was quantified by spectrophotometry and its size integrity verified by gel electophoresis. Defolliculated stage IV and V oocytes from *Xenopus laevis* were injected with 10 ng KCNQ1 or KCNQ4 cRNA with or without 2 ng MinK or MiRP2 cRNA.

Electrophysiology

Whole-cell currents in oocytes were recorded at room temperature by two-electrode voltage clamp (TEVC) using an OC-725C Amplifier (Warner Instruments) and an IBM computer running pClamp9 software (Axon Instruments). Pipettes were filled with 3 M KCl and had a 0.5–1.0 MΩ resistance. Bath solution was (in mM) 4 KCl, 96 NaCl, 0.7 $MgCl_2$, 1 $CaCl_2$, 10 HEPES (pH 7.6 with NaOH). HMR1556 (Aventis) was added to the bath solution to give a final concentration of 10 μM, from a 10 mM stock solution in dimethyl sulfoxide. Experiments were performed 3–4 d after cRNA injection. Oocytes were held at −80 mV, stepped for 3 s at voltages between −120 mV and +60 mV in 20-mV steps, and then held for a 1-s tail pulse at −30 mV before returning to the holding potential. For assessment of slowly deactivating mutants, the voltage "family" was preceded by activation at +60 mV and then either a 1-s pulse to −80 mV, or a 40-s pulse to −120 mV. Current–voltage relationships were obtained by measuring current at the end of 3-s depolarizing pulses unless otherwise indicated. Conductance was obtained by measuring the tail current at −30 mV immediately following the prepulse. Normalized conductance–voltage (G/V) relationships were fitted using the Boltzmann equation ($G = G_{max}/[1 + \exp(V - V_{1/2}/k)]$, where $V_{1/2}$ = half-maximal activation and k = slope factor, and values reported where informative. Data analysis was performed using CLAMPFIT 9 (Axon Instruments), EXCEL 5.0 (Microsoft), and ORIGIN 6.0 (Microcal). Data are expressed as mean ± SEM, with n specifying the number of independent experiments.

Structural Models

Homology modeling of the KCNQ1 S4 and S4–S5 linker domains (Fig. 11) was performed with the SWISS-MODEL program (Schwede et al., 2003) using structural coordinates from X-ray crystallographic studies of similar domains in Kv1.2 as a template (Long et al., 2005). Images were prepared using PROTEIN EXPLORER ALPHA.

Online Supplemental Material

Fig. S1 (available at http://www.jgp.org/cgi/content/full/jgp.200609612/DC1) illustrates raw and normalized current–voltage relationships for wild-type, R228A, R231A, and R237A KCNQ1 channels.

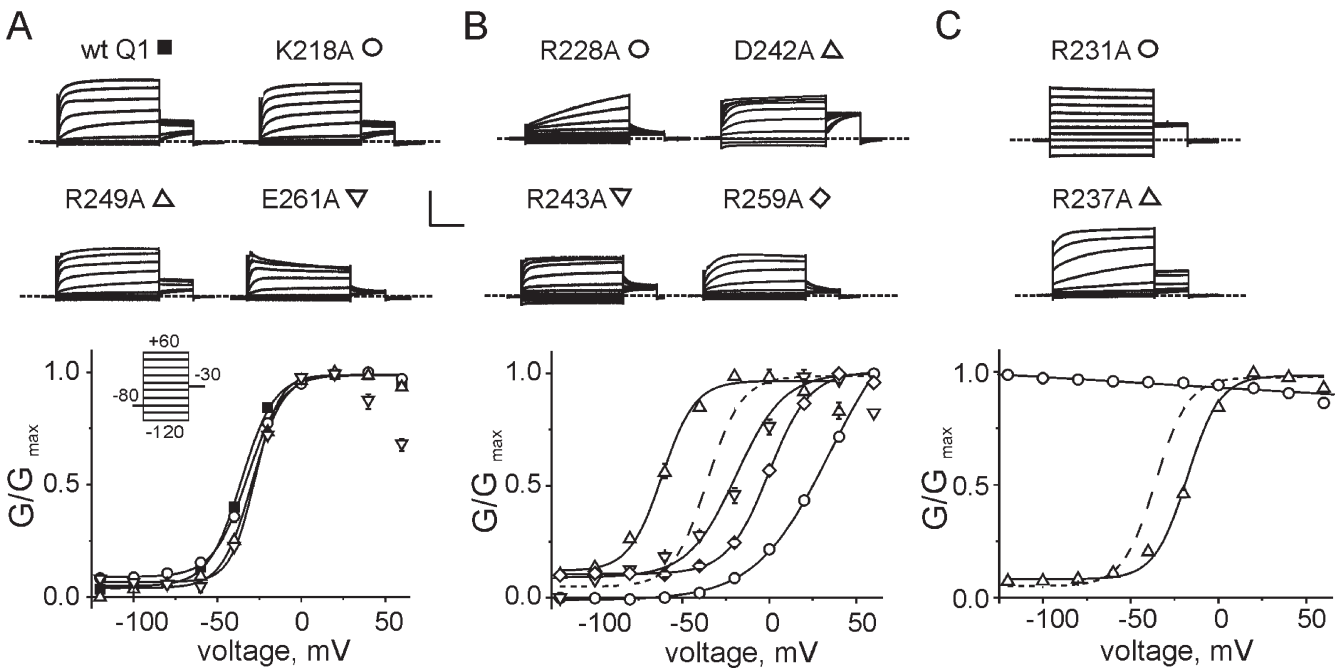

Figure 2. Effects of S4 alanine scanning mutagenesis on homomeric KCNQ1 channel activation. (A–C) Top, exemplar current traces recorded in oocytes expressing wild-type (wt) or alanine mutant KCNQ1 (Q1) channels as indicated, grouped according to their effects on $V_{1/2}$ of activation (see text for details). Currents were recorded by TEVC using the standard voltage family protocol (inset, A). Bars: vertical, 1 μA (wt Q1, K218A, R259A, R231A), 0.5 μA (R249A, E261A, R228A, D242A, R243A,), 2 μA (R237A); horizontal, 1 s. Zero current level indicated by dashed line. Bottom, normalized G/V relationships obtained by measuring the tail current immediately following the prepulse; n = 9–22. In B and C dashed lines represent wt Q1 for reference. Error bars indicate SEM. Data were fitted with the Boltzmann equation ($V_{1/2}$ and k values in Table I).

RESULTS

KCNQ1 is a Kv channel α subunit in the S4 superfamily of voltage-gated ion channels. Each KCNQ1 α subunit bears six transmembrane helices with the fourth, S4, being considered the principal component of voltage sensing (Fig. 1 A). MiRPs are predicted to span the membrane once (Fig. 1 A). Here, alignment of S4 domains from all known eukaryotic voltage-gated cation channel α subunits revealed a unique paucity of net positive charge (+3) in the KCNQ1 S4, compared with +7 in *Shaker*, +5 in other KCNQ channels, +6 in HCN channels, and at least +5 in voltage-gated sodium and voltage-gated calcium channels (subset in Fig. 1 B; S4 domain as defined in Aggarwal and MacKinnon, 1996, see Discussion). In particular, the CO_2H half of KCNQ1 S4 (residues 238–248) is electroneutral, whereas in *Shaker* and Kv1.1 this region has a net charge of +3 (Fig. 1 B).

Based on this unique KCNQ1 S4 charge balance, we first asked whether S4 constitutes the major component of the KCNQ1 voltage sensor as it does in other Kv channels. Each of the charged residues in the S3–S4 linker, S4, and S4–S5 linker (red domains in Fig. 1 A) of KCNQ1 were sequentially replaced with alanine. The resultant mutant channels were expressed in *Xenopus* oocytes and their functional properties studied using TEVC. Substitution of each of several charged residues (K218, R249, and E261) had no significant effect on the voltage dependence of KCNQ1 activation, although the E261A mutation increased the extent of inactivation (Fig. 2 A; Table I). Substitution of several other basic residues (R228A, R243A, and R259A) induced a positive shift in the voltage dependence of activation, while substitution of the S4 acidic residue D242 induced a negative shift in the voltage dependence of activation (Fig. 2 B; Table I). Substitution of either of the two other S4 basic residues (positions R231 and R237) produced channels with unexpected behavior. Homomeric R231A-KCNQ1 channels were constitutively open, with a linear G/V relationship (Fig. 2 C), a finding not observed with previous single amino acid substitutions in S4 of *Shaker* or hERG Kv channels (Aggarwal and MacKinnon, 1996; Piper et al., 2005). R237A channels showed a right shifted voltage dependence of activation and appeared to accumulate in the open state with the standard voltage "family" protocol (Fig. 2 C). This accumulation was even more evident when using a protocol with prior activation to +60 mV followed by a 1-s pulse to −80 mV before the voltage family (Fig. 3, A and C). A longer (40 s) holding pulse to −120 mV before the voltage family revealed that the accumulation in the open state of R237A channels was due to extremely slow

TABLE I

Effects of Charge Removal on the Voltage Dependence of Homomeric KCNQ1 Activation

Channel	$V_{1/2}$, mV	*k*, mV	*n*
wt KCNQ1	−35.67 ± 0.53	9.29 ± 0.43	14
K218A	−31.54 ± 0.96	10.18 ± 0.46	12
R228A	+36.14 ± 2.20	24.97 ± 3.4	14
R231A	NA	NA	22
R237A	−17.59 ± 1.42	10.33 ± 1.29	14
D242A	−62.69 ± 3.38	10.40 ± 3.08	9
R243A	−19.59 ± 4.97	14.78 ± 4.5	11
R249A	−29.39 ± 1.23	8.89 ± 0.95	13
R259A	−1.04 ± 0.96	11.2 ± 0.86	21
E261A	−28.27 ± 1.94	7.38 ± 1.36	10

Voltage dependence of current activation for homomeric wild-type (wt) KCNQ1 channels or those with alanine substituted for charged residues at positions indicated. Conductance–voltage relationships were fit to Boltzmann distributions to derive values for the midpoint of activation ($V_{1/2}$) and slope (*k*) of the curves. *n* = number of independent experiments; NA = not applicable.

deactivation (τ = 4650 ± 305 ms at −120 mV; *n* = 5); if sufficient deactivation time was allowed between pulses, these channels showed a similar voltage dependence and rate of activation to that of wild-type channels (Fig. 3, B and C).

To confirm that the leak current observed with R231A-KCNQ1 was attributable to movement of K^+ ions through the pore of this channel, the raw I/V curve was plotted and shown to reverse at ∼−80 mV, as expected for a K^+-selective channel under our experimental conditions (Fig. 4 A). Furthermore, R231A-KCNQ1 channel current was inhibited by HMR1556, a relatively KCNQ1-specific pore blocker (Lerche et al., 2000), to a similar extent to that of wild-type KCNQ1 (Fig. 4, B and C). Taken together, the data show that unlike other Kv channels, homomeric KCNQ1 channels can be relatively easily switched to a constitutively open state, by loss of a specific single charge in the N-terminal half of S4.

These findings suggested that S4 charge balance is a dominant factor in determining the propensity to form leak, and predicted that leak properties would be conferred to other voltage-gated ion channels by adoption of an S4 charge balance similar to that of R231A-KCNQ1. To test this, we mutated the S4 domain of related α subunit KCNQ4, which has two more basic residues than KCNQ1 in the CO_2H-terminal half of S4. Removing these additional charges in KCNQ4 S4 (positions 216 and 220) in the context of an R207A mutation (to mimic the R231A-KCNQ1 S4 domain, referred to as tm-KCNQ4) produced a leak channel, with voltage- and time-independent activation (Fig. 5, A–C). Thus, as for KCNQ1, the KCNQ4 S4 domain is stable in the "on" position even at hyperpolarized voltages if a charge pattern resembling that of R231A-KCNQ1 S4 is imposed on KCNQ4 S4, suggesting the propensity for leak is determined by S4 charge and not the KCNQ1 pore.

The contrasting effects of MinK and MiRP2 on KCNQ1 activation are striking given that only subtle differences have been found in their interaction with the KCNQ1 S6 pore-lining domain (Melman et al., 2002, 2004; Panaghie et al., 2006). Further, MinK, MiRP1, and MiRP2 interact with a variety of other ion channel α subunits (at least 10 between them) without inducing constitutive current (McCrossan and Abbott, 2004). These previous findings, together with observations here that KCNQ1 S4 determines a unique propensity for constitutive activation, suggested the possibility that KCNQ1 S4 is critical in determining the relative effects on activation of different ancillary subunits, and predicted that S4 charge balance might determine the effects of MinK on KCNQ1 activation. Indeed, three

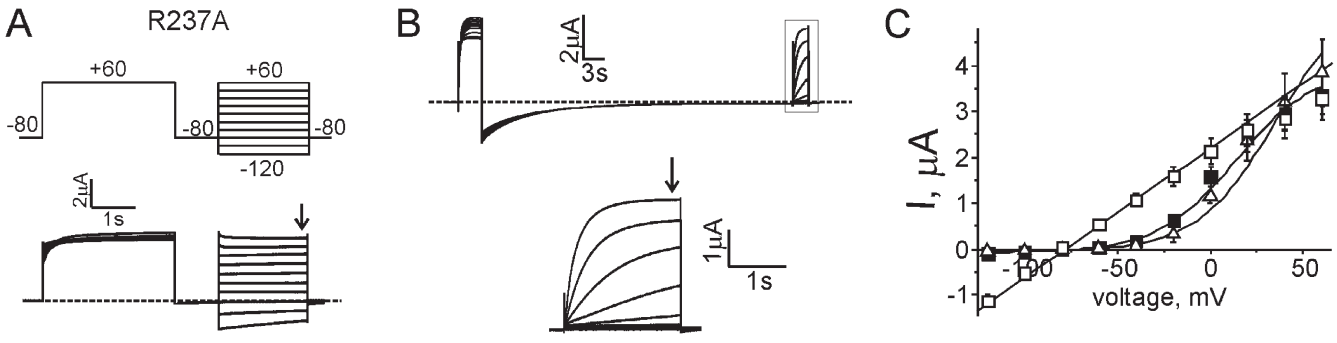

Figure 3. Homomeric R237A-KCNQ1 channels deactivate slowly. (A) Exemplar current trace recorded in oocytes injected with R237A-KCNQ1 (Q1) cRNA using a voltage protocol including a depolarizing prepulse followed by a standard voltage family (top). Zero current level indicated by dashed line. (B) Top, exemplar current trace recorded as in A but using a modified protocol with a 40-s hyperpolarizing step at −120 mV before the voltage family. Zero current level indicated by dashed line. Bottom, expanded view of boxed region from trace above. (C) Raw IV relationships measured at the time points indicated by the arrows in A and B (open squares and triangles respectively); *n* = 5–7. For comparison, the IV relationship for R237A currents recorded using the standard voltage protocol in Fig. 2 (without prior depolarization) is also included (filled squares). Error bars indicate SEM.

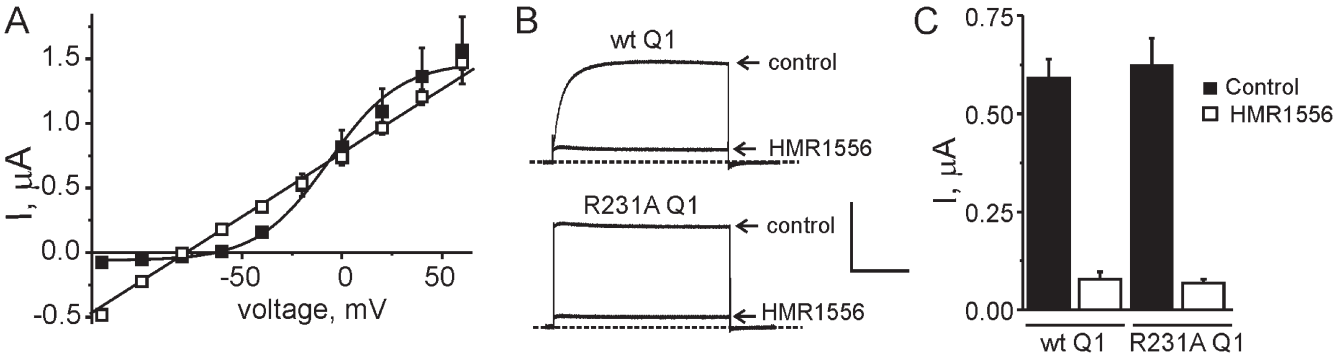

Figure 4. Properties of the R231A-KCNQ1 leak current. (A) Raw I/V relationships for wild-type KCNQ1 (Q1) (filled squares) and R231A-Q1 (open squares) obtained by measuring the peak current at the end of 3-s voltage steps, for oocytes as in Fig. 2, A and C. (B and C) Effects of Q1 pore blocker HMR1556 on R231A-Q1 current. (B) Exemplar current traces from oocytes injected as indicated and stepped to 0 mV for 3 s from a holding voltage of −80 mV before (control) and after (HMR1556) a 2-min perfusion with 10 μM HMR1556. Bars: vertical, 0.5 μA; horizontal, 1 s. Zero current level indicated by dashed lines. (C) Mean raw current measured at the end of the 3-s depolarizing pulse from traces as in B; $n = 8$.

of the KCNQ1 S4 mutants produced atypical currents when coexpressed with MinK, whereas the remaining mutants produced voltage-dependent channels with slow activation similar to wild-type I_{Ks} as quantified by the G/V relationships and the time to reach half maximal current at +60 mV (Fig. 6).

Of the S4 charges, alanine substitution at positions K218, D242, and R243 had no significant effects on the voltage dependence or kinetics of MinK-KCNQ1 channel activation (Fig. 6, A and D). R231A-KCNQ1 remained a leak channel but expressed ~20-fold higher current density with MinK, indicating interaction of MinK with KCNQ1, but dominance of activation gating by the mutant S4 domain (Fig. 6, B and D). R228A-KCNQ1 channels showed left-shifted voltage-dependent activation (Fig. 6 B) and sevenfold shorter rise time to half-maximal activation compared with wild-type MinK-KCNQ1 channels (Fig. 6 D) and appeared to accumulate in the open state using the standard protocol; this mutant is described further below (Fig. 7). R237A-KCNQ1, which activated like wild-type KCNQ1 but deactivated slowly in its homomeric form, formed a classic leak channel when coexpressed with MinK (Fig. 6, B and D). In the S4–S5 linker, alanine substitution of either R259 or E261 produced a positive shift in the voltage dependence of activation and a slowing of activation in MinK-KCNQ1 channels, whereas R249A channels behaved like wild-type channels in both aspects (Fig. 6, C and D). Thus, loss of positive charge at positions 231 or 237 was sufficient to override the effects of MinK, either retaining or inducing additional constitutive current.

Channels formed by coexpression of MinK and R228A-KCNQ1 channels were analyzed further using a +60-mV prepulse before the voltage family, resulting in an increase in instantaneous current at all voltages (Fig. 7 A). This suggested that slow deactivation was allowing R228A channels to accumulate in the open state, a hypothesis borne out by data generated using an alternative protocol with a much longer interpulse interval, revealing that MinK-R228A-KCNQ1 channels exhibited a $\tau_{deactivation}$ of 1148 ± 276 ms at −120 mV ($n = 5$) (Fig. 7 B). The longer recovery phase permitted full deactivation before the voltage family, resulting in currents with negligible instantaneous current, slow activation, and

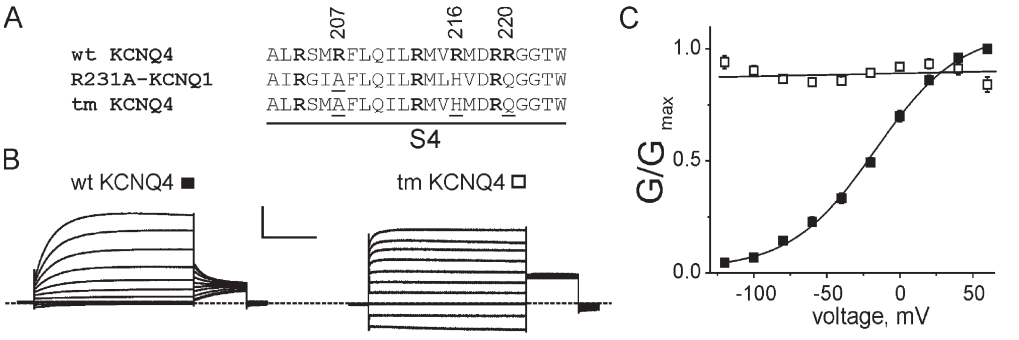

Figure 5. Charge paucity in KCNQ4 S4 confers constitutive activation. (A) S4 sequence alignment for wild-type (wt) and triple mutant (tm) KCNQ4 versus R231A-KCNQ1. Positively charged amino acids are indicated in bold; mutated resides are underlined. (B) Exemplar current traces recorded in oocytes injected with wt or tm KCNQ4 mutant as indicated. Bars: vertical, 1 μA for wt KCNQ4 and 0.3 μA for tm KCNQ4; horizontal, 1 s. Zero current level indicated by dashed lines. (C) Mean G/V relationships for oocytes as in B obtained by measuring the tail current immediately following the prepulse; $n = 10$–13. Data for wt KCNQ4 were fitted with the Boltzman equation: $V_{1/2} = -16.7 \pm 2.2$ mV, $k = 28.0 \pm 1.8$ mV.

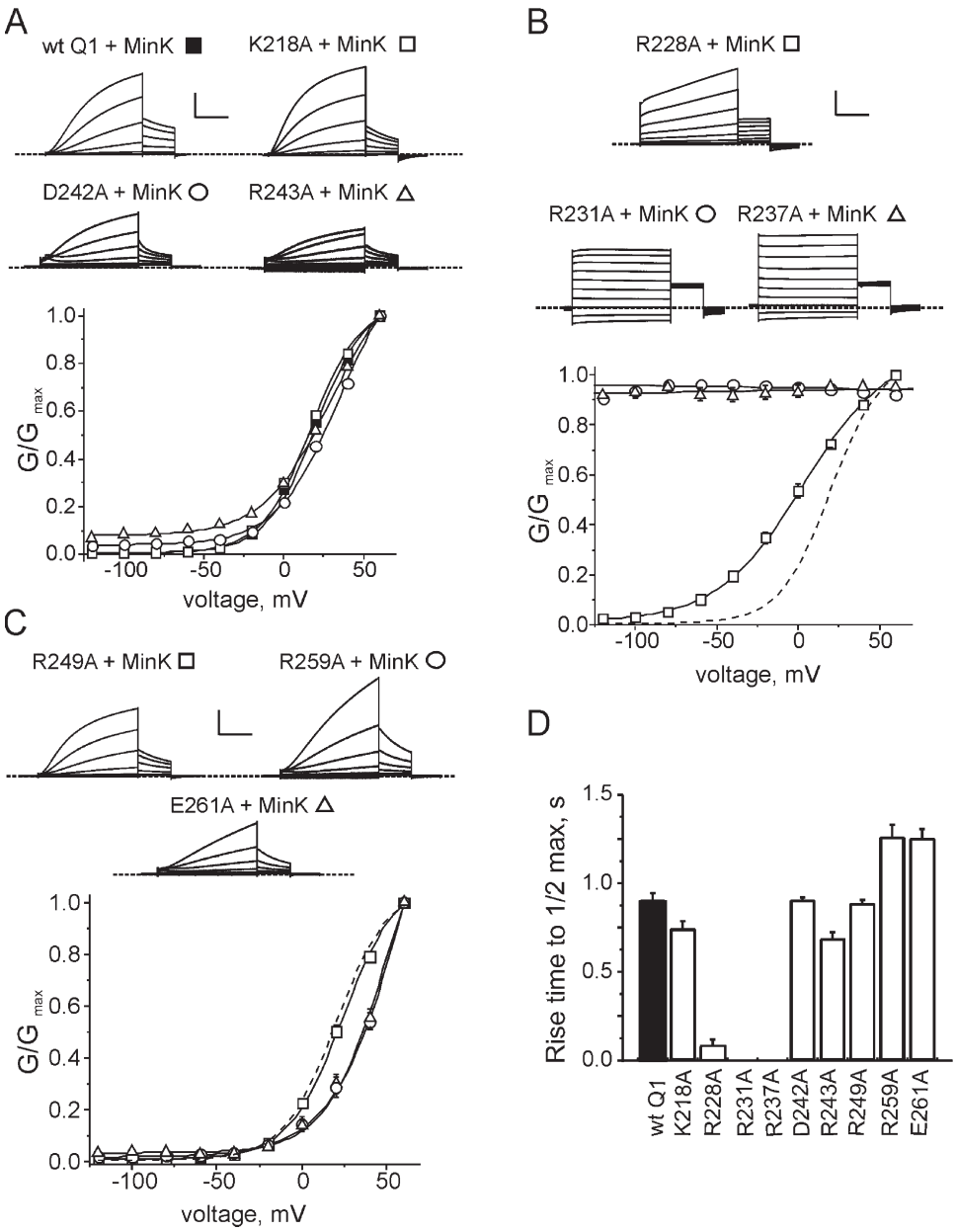

Figure 6. S4 charge balance dominates the attributes of MinK-KCNQ1 activation. (A) Top, exemplar current traces recorded in oocytes coexpressing wild-type or mutant KCNQ1 (Q1) channels as indicated and MinK. Currents were recorded by TEVC using the standard voltage family protocol (Fig. 2 A). Bars: vertical, 0.5 μA (D242A, R243A), 4 μA (wt Q1, K218A); horizontal, 1 s. Bottom, normalized G/V relationships obtained by measuring the tail current immediately following the prepulse; n = 10–13. Error bars indicate SEM. In all panels, voltage-dependent activation data were fitted with a sigmoidal relationship. (B) Top, exemplar current traces recorded in oocytes coexpressing mutant KCNQ1 (Q1) channels as indicated and MinK. Currents were recorded by TEVC using the standard voltage family protocol (Fig. 2 A). Bars: vertical, 2 μA (R231A), 4 μA (R237A), 6 μA (R228A); horizontal, 1 s. For R231A channels, a 10-fold dilution of cRNA was required to prevent excessive current density. Bottom, normalized G/V relationships obtained by measuring the tail current immediately following the prepulse; n = 6–10. Dashed line represents wt Q1 + MinK for reference. Error bars indicate SEM. (C) Top, exemplar current traces recorded in oocytes coexpressing mutant KCNQ1 (Q1) channels as indicated and MinK. Currents were recorded by TEVC using the standard voltage family protocol (Fig. 2 A). Bars: vertical, 0.5 μA (R259A, E261A), 2 μA (R249A); horizontal, 1 s. Bottom, normalized G/V relationships obtained by measuring the tail current immediately following the prepulse; n = 8–10. Dashed line represents wt Q1 + MinK for reference. Error bars indicate SEM. (D) Activation kinetics expressed as time to reach half-maximal current at +60 mV, for oocytes in A–C; n = 6–13. Error bars indicate SEM.

right-shifted, voltage-dependent activation compared with wild-type channels (Fig. 7, B and C).

These findings posed the question of the relative role of the KCNQ1 S4 domain in channels formed by coassembly of KCNQ1 with MiRP1 or MiRP2; here we focused on the latter, which gives more robust currents with KCNQ1. In voltage-dependent ion channels S4 is thought to move upon membrane depolarization; this movement is then transmitted to the channel gate via the S4–S5 linker to cause channel opening (Fig. 8 A). In MiRP2-KCNQ1 channels the gate is constitutively open regardless of voltage, suggesting one of two models: either the gate is always locked open and uncoupled from S4 movement (Fig. 8 B, left) or alternatively S4 is always locked in the active state and its position is still communicated to the gate via the S4–S5 linker (Fig. 8 B, right). When coexpressed with MiRP2, all KCNQ1 S4 mutants retained some constitutive activation as assessed from tail current after the −120-mV pulse, but the relative contribution of this constitutive component was altered, varying between 20 and 100% of the total current (Fig. 8, C and D). Alanine substitution of basic residues increased the fraction of constitutive current in only two cases, at positions R231 or R237; D242A

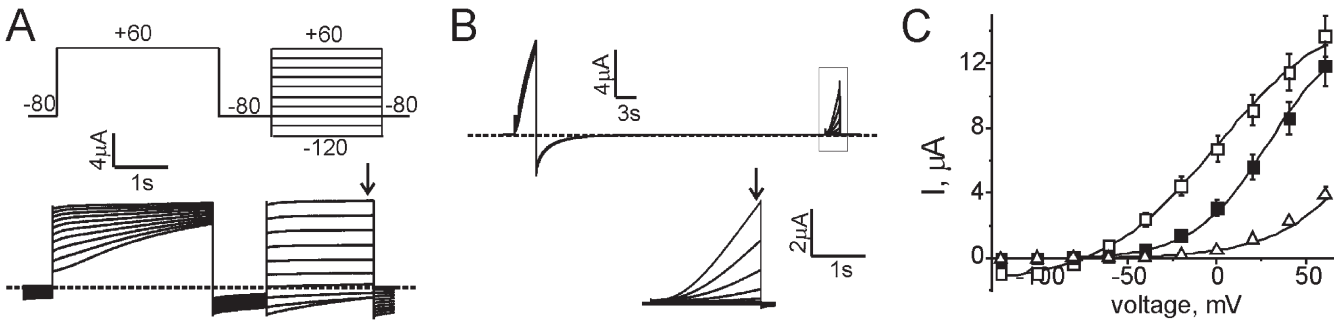

Figure 7. MinK-R228A-KCNQ1 channels deactivate slowly. (A) Exemplar current trace recorded in oocytes injected with R228A-KCNQ1 and MinK cRNA using the indicated voltage protocol (top). Zero current level indicated by dashed line. (B) Top, exemplar current trace recorded in oocytes injected with R228A-KCNQ1 and MinK cRNA using a modified version of the voltage protocol in A, with a 40-s hyperpolarizing step at −120 mV before the voltage family. Zero current level indicated by dashed line. Bottom, expanded view of boxed region from trace above. (C) Raw I/V relationships measured at the time points indicated by the arrows in A and B (open squares and triangles respectively); $n = 5–6$. For comparison, the I/V relationship for R228A + MinK currents recorded using the standard voltage protocol in Fig. 2 A (without prior depolarization) is also included (filled squares). Error bars indicate SEM.

substitution (an increase in net positive charge) also produced an increase in constitutive current (Fig. 8 C). Neutralization of R228, R243, or R249 reduced constitutive current two to threefold (Fig. 8 D). Two of the KCNQ1 S4–S5 linker mutants, R259A and E261A, formed predominantly voltage-dependent channels with MiRP2; differences in their G/V relationships depending upon MiRP2 coexpression indicated these mutant KCNQ1 subunits still coassembled with MiRP2 (Fig. 8 E). Current–voltage relationships for key KCNQ1 mutants alone and with MinK or MiRP2 are illustrated for comparison in Fig. S1 (available at http://www.jgp.org/cgi/content/full/jgp.200609612/DC1).

These data support an active role for the voltage sensor in MiRP2-KCNQ1 channels because if MiRP2 directly locked open the KCNQ1 channel gate without communication between the gate and S4, one would not expect the KCNQ1 S4 charge balance to determine the relative proportion of leak in MiRP2-KCNQ1 channels. The results are thus consistent with the "S4 locked on" model (Fig. 8 B, right), suggesting a model in which both KCNQ1 S4 charge balance and sequence differences between MinK and MiRP2 dictate the relative gating effects of MinK and MiRP2. S4–S5 linker charges also influenced constitutive activation in MiRP2-KCNQ1 channels, either by communicating S4 position to the activation gate or, alternatively, by mediating functional interaction (but not coassembly per se) between MiRP2 and KCNQ1.

The inability of MiRP1 and MiRP2 to convert other channels to leak mode is especially striking given the close similarity between KCNQ1 and other KCNQ subunits with which MiRP1 and MiRP2 interact. KCNQ2–5 subunits each bear two more basic residues than KCNQ1 in an otherwise highly homologous S4 (Fig. 9 A). KCNQ2 is regulated by MiRP1; KCNQ4 is regulated by MiRP2; neither pairing results in constitutive activation (Schroeder et al., 2000b; Tinel et al., 2000b). Based on the results in Fig. 8, we hypothesized that the propensity of homomeric KCNQ1 channels to form leak channels after NH_2-end S4 charge removal and the ability of MiRP2 to impose leak properties upon wild-type KCNQ1 are related phenomena arising from native KCNQ1 S4 charge paucity at the CO_2H end. To test this hypothesis, two approaches were adopted. First, charge was added to KCNQ1 S4 and effects of MiRP2 analyzed (Fig. 9, B–D). Charge addition either left shifted activation of homomeric KCNQ1 channels (H240R or H240R,Q244R mutants) or increased the constitutive current (Q244R) (Fig. 9, B–D) compared with wild-type homomeric KCNQ1 channels (Fig. 2). The opposite was observed for MiRP2-KCNQ1 channels; addition of positive charge reduced constitutive current from 80% of maximal to 10% of maximal (H240R and H240R,Q244R channels; Fig. 9, B and D) or to 70% of maximal (Q244R; Fig. 9 C). None of the mutants prevented coassembly with MiRP2, as evidenced by changes in the G/V slope and/or voltage dependence, or an increase in constitutive current, compared with homomeric mutant channels (Fig. 9, B–D). These findings strongly suggested that the unique charge balance of the KCNQ1 S4 domain is required for removal of voltage dependence by MiRP2. Specifically, the charge paucity of the CO_2H-terminal half (effectively neutral, containing one negative and one positive charge) is required for constitutive activation of MiRP2-KCNQ1, with H240R substitution being most deleterious to function. In a further experiment, introduction of an arginine at position 234 in the N terminus of KCNQ1 S4, to restore the third of four charges known to be critical for activation gating and gating current in the *Shaker* potassium channel (Aggarwal and MacKinnon, 1996) resulted in nonfunctional channels (unpublished data). One possible explanation of this is that the Q234R mutation locks S4 "off" (with or without MiRP2), although it is also possible that this mutation prevents channel function by other mechanisms such as trafficking deficiency.

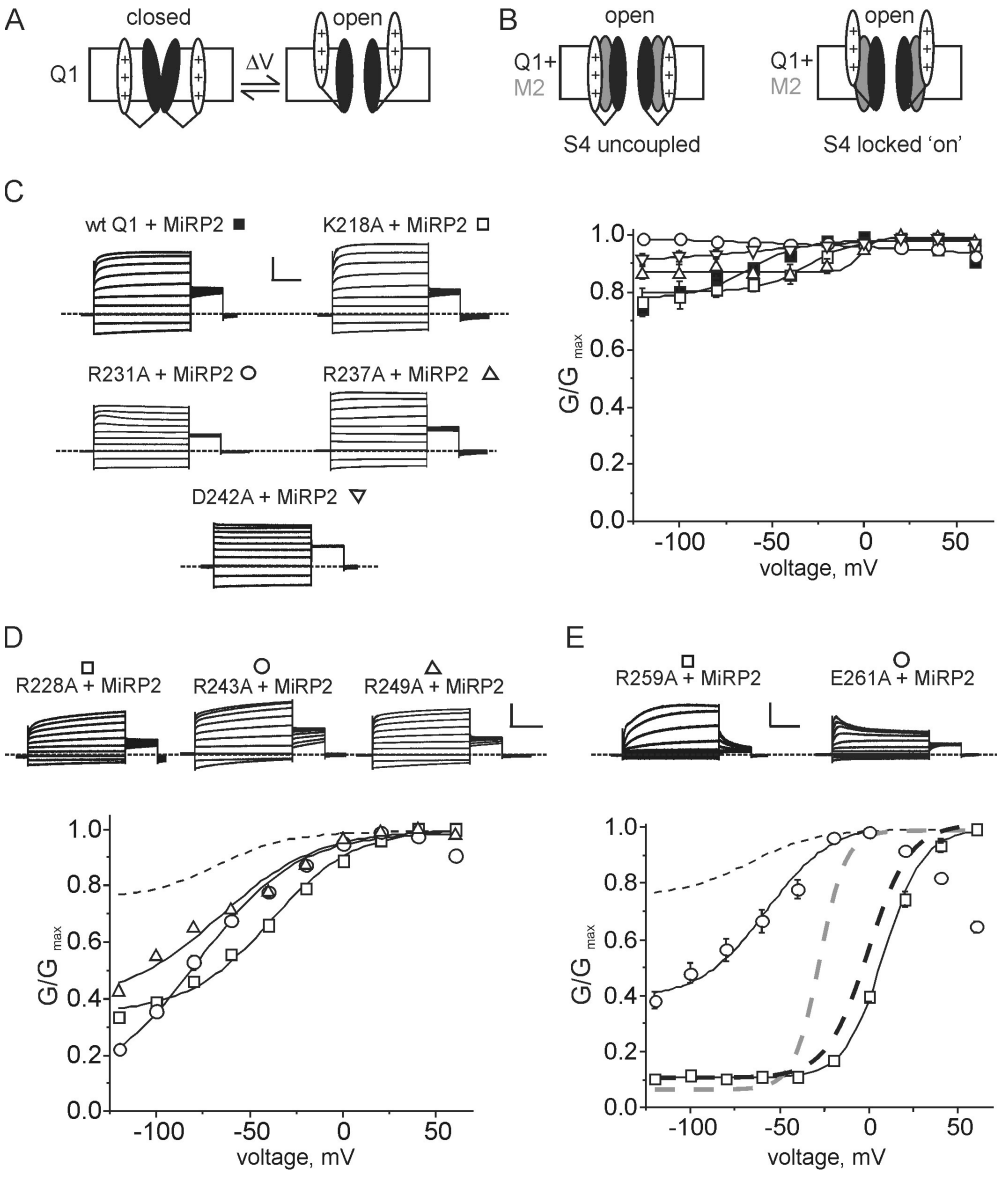

Figure 8. Net charge of S4 and the S4–S5 linker determines extent of constitutive activation of MiRP2-KCNQ1 channels. (A and B) Alternative models to explain (A) the voltage dependence of homomeric KCNQ1 channels versus (B) the voltage independence of MiRP2-KCNQ1 channels. The lipid bilayer is shown in white, with the extracellular side uppermost. (A) In homomeric KCNQ1 channels, the S4 (white with plus signs for net positive charge) is in the down (off) position and thus the gate (black) is closed (left) until depolarization shifts the S4 to the up (on) position, which opens the gate via the S4–S5 linkers (black lines) (right). (B) In MiRP2-KCNQ1 channels, MiRP2 is shown in gray. The gate is always open even at hyperpolarized voltages either because the S4 position is not communicated to the gate (left, S4 uncoupled) or because the S4 is always in the up (on) position regardless of membrane potential (right, S4 locked on). (C) Left, exemplar current traces recorded in oocytes coexpressing wild-type MiRP2 and wild-type or mutant KCNQ1 (Q1) channels as indicated. Currents were recorded by TEVC using the standard voltage family protocol (Fig. 2 A). Bars: vertical, 1 μA except 4 μA for R237A; horizontal, 1 s. Zero current level indicated by dashed lines. Right, normalized G/V relationships obtained by measuring the tail current immediately following the prepulse; n = 6–13. Error bars indicate SEM. Data were fitted with either a straight line or a sigmoidal relationship. (D) Top, exemplar current traces recorded in oocytes coexpressing wild-type MiRP2 and mutant KCNQ1 (Q1) channels as indicated. Currents were recorded by TEVC using the standard voltage family protocol (Fig. 2 A). Bars: vertical, 1 μA except 0.5 μA for R243A; horizontal, 1 s. Zero current level indicated by dashed line. Bottom, normalized G/V relationships obtained by plotting the tail current immediately following the prepulse versus prepulse voltage; n = 10–15. Error bars indicate SEM. Dashed line indicates G/V relationship for wild-type MiRP2-KCNQ1 channels for comparison. Data were fitted with a sigmoidal relationship. (E) Top, exemplar current traces recorded in oocytes coexpressing MiRP2 with either of two S4–S5 linker KCNQ1 mutants as indicated. Bars: vertical, 0.5 μA (R259A) and 0.4 μA (E261A); horizontal, 1 s. Zero current level indicated by dashed line. Bottom, normalized G/V relationships obtained by plotting the tail current immediately following the prepulse versus prepulse voltage; n = 11. For comparison, G/V relationships for oocytes injected with R259A alone (thick black dashed line), E261A alone (gray dashed line), and wt KCNQ1 + MiRP2 (thin black dashed line) are also shown. Error bars indicate SEM. A Boltzmann fit of the G/V relationship for R259A Q1 + MiRP2 gave $V_{1/2} = -56.3 \pm 3.3$ mV; $k = 3.6 \pm 1.8$ mV. Meaningful quantitative fitting of the E261A G/V relationship was prevented by some constitutive activation and subsequent inactivation.

Second, the converse approach was also taken to explore the role of S4 charge balance in modulation by MiRP2, with removal of charges from KCNQ4 S4 (R216 and R220) and KCNQ2 (R210 and R214; Fig. 10 A), and coexpression of MiRP2. KCNQ2 channels with a single R210H mutation, or double R210H, R214Q mutation were nonfunctional with or without MiRP2, as were single mutant R220Q-KCNQ4 channels (unpublished data). The functional properties of wild-type KCNQ2 were not affected by MiRP2; neither were the properties

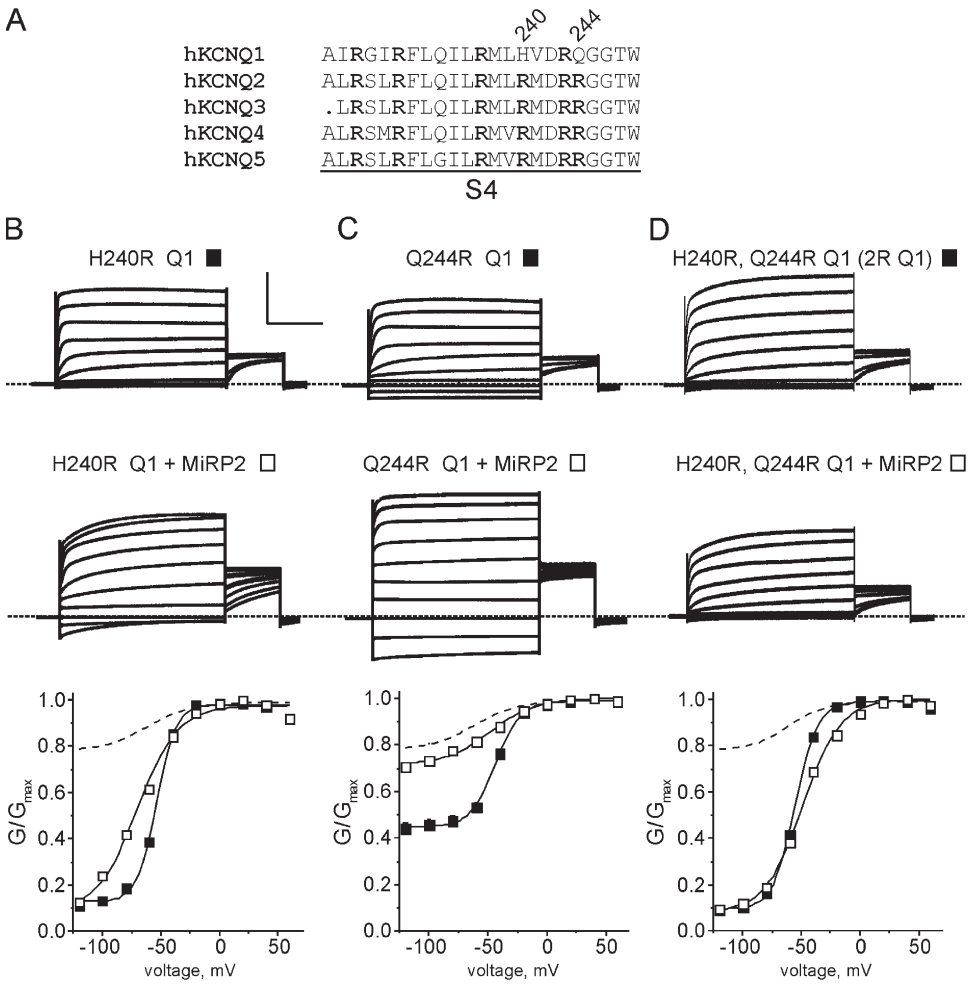

Figure 9. Charge paucity in the CO_2H-terminal end of S4 is required for constitutive activation of MiRP2-KCNQ1 channels. (A) S4 sequence alignment for the KCNQ family. Positively charged amino acids are indicated in bold; KCNQ1 lacks positive charges at positions 240 and 244, which are present at equivalent positions in KCNQ2–5. (B–D) Top, exemplar current traces recorded in oocytes injected with KCNQ1 (Q1) variants: (B) H240R Q1, (C) Q244R Q1, or (D) H240R, Q244R Q1 (2R Q1) alone or with MiRP2 as indicated. Bars: vertical, 1 μA; horizontal, 1 s. Zero current level indicated by dashed lines. Bottom, mean normalized G/V relationships for oocytes injected with (B) H240R Q1, (C), Q244R Q1, or (D) H240R, Q244R Q1 (2R Q1) alone (filled squares) or with MiRP2 (open squares); n = 10–15. Dashed lines indicate G/V relationship for wild-type MiRP2-KCNQ1 channels for comparison. Error bars indicate SEM. G/V relationships when constitutive activation was <20% were fitted with the Boltzmann equation. Values were as follows: H240R Q1, $V_{1/2} = -53.5 \pm 0.5$ mV, $k = 8.2 \pm 0.5$ mV; H240R Q1 + MiRP2, $V_{1/2} = -69.0 \pm 3.4$ mV, $k = 17.9 \pm 2.8$ mV, (significant difference in $V_{1/2}$ with/without MiRP2; $P < 0.001$). 2R Q1, $V_{1/2} = -54.88 \pm 0.49$ mV, $k = 9.6 \pm 0.3$ mV; 2R Q1 + MiRP2, $V_{1/2} = -48.46 \pm 0.6$ mV, $k = 16 \pm 0.5$ mV (significant difference in k with/without MiRP2; $P < 0.001$).

of R214Q-KCNQ2, which showed a +25- mV shift in the voltage dependence of activation compared with wild-type KCNQ2, with or without MiRP2 (Fig. 10, B and C). These data suggest a lack of functional interaction of KCNQ2 with MiRP2 and act as a negative control, showing a lack of introduction of constitutive current by MiRP2 in each case.

Coexpression of wild-type KCNQ4 with MiRP2 resulted in a sixfold reduction of KCNQ4 current amplitude, similar to that previously reported (Schroeder et al., 2000b). A similar reduction was observed for double mutant R216H, R220Q-KCNQ4, while R216H-KCNQ4 current was reduced twofold by MiRP2 (Fig. 10 D). Effects of MiRP2 on the proportion of constitutively active KCNQ4 current were quantified by measuring tail current and plotting normalized tail current versus prepulse voltage for wild-type and mutant KCNQ4 channels without and with MiRP2 (Fig. 10 E, top and bottom, respectively). Homomeric double mutant R216H, R220Q-KCNQ4 channels showed 20% constitutive tail current after a −120-mV prepulse, compared with essentially none in wild-type or R216H-KCNQ4; both homomeric mutant channels showed a positive shift in the voltage dependence of the nonconstitutive current compared with wild-type homomeric KCNQ4 (Fig. 10 E, top). In channels formed with MiRP2, R216H-KCNQ4 showed 20% of maximal tail current after a −120-mV prepulse compared with zero tail current after the −120 mV prepulse in channels formed with MiRP2 and wild-type KCNQ4. Most significantly, MiRP2 increased the tail current of double mutant R216H, R220Q-KCNQ4 channels from 20% of maximal to 75% of maximal after a prepulse of −120 mV (Fig. 10 E, bottom).

These data demonstrated that imposing the wild-type KCNQ1 S4 charge balance on KCNQ4 enabled conversion to leak by MiRP2, just as mutagenesis of KCNQ4 S4 to mimic that of R231A-KCNQ1 had resulted in constitutive activation of homomeric triple mutant KCNQ4 channels (Fig. 5). While we could not directly compare one of the complementary sets of single S4 mutants shown in Figs. 9 and 10 (H240R-KCNQ1 with R220Q-KCNQ4) because of the lack of functional expression of

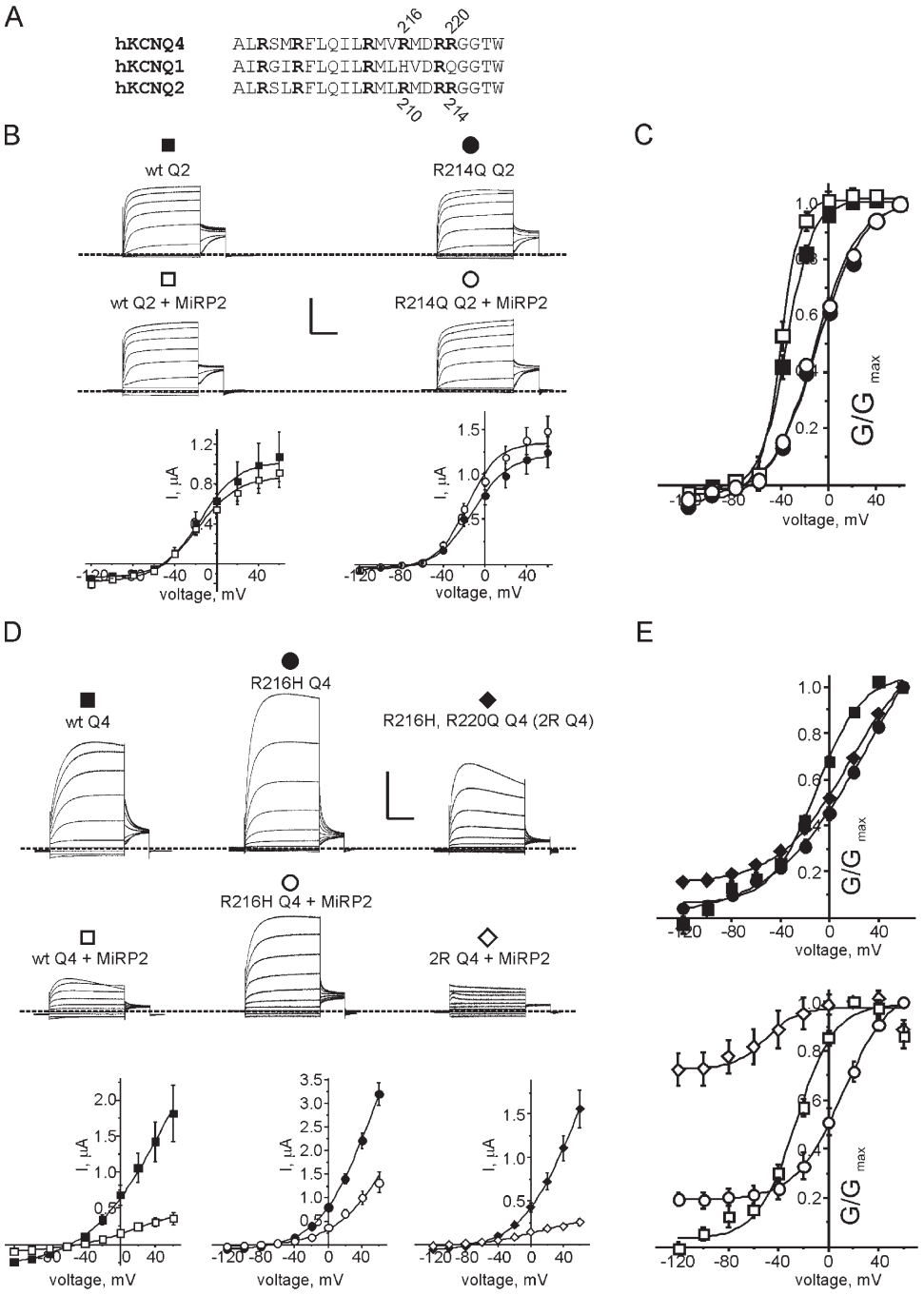

Figure 10. Charge paucity in the CO_2H-terminal end of S4 endows constitutive activation upon MiRP2-KCNQ4 channels. (A) S4 sequence alignment for KCNQ1, 2, and 4. Basic amino acids are indicated in bold; KCNQ1 lacks positive charges at positions 240 and 244; these are present at equivalent positions in KCNQ2 and 4 (numbered accordingly) and were mutated to mimic the KCNQ1 S4 for experiments in B–E. (B) Top, exemplar current traces recorded in oocytes injected with wild-type (wt) or R214Q KCNQ2 (Q2) alone or with MiRP2 as indicated. Bars: vertical, 0.5 μA; horizontal, 1 s. Zero current level indicated by dashed lines. Bottom, mean I/V relationships for oocytes as above; n = 8–11. Error bars indicate SEM. (C) Mean G/V relationships for oocytes injected as in B, symbols as in B; n = 8–11. Error bars indicate SEM. Data were fitted with the Boltzmann equation; values were as follows: wild-type Q2, $V_{1/2}$ = −36.2 ± 1.4 mV, k = 11.0 ± 1.0 mV, A1 = −0.01 ± 0.01, A2 = 1.0 ± 0.01; wild-type Q2 + MiRP2, $V_{1/2}$ = −40.8 ± 1.4 mV, k = 8.0 ± 1.3 mV, A1 = −0.02 ± 0.01, A2 = 1.02 ± 0.01; R214Q-Q2, $V_{1/2}$ = −11.1 ± 1.0 mV, k = 20.1 ± 0.9 mV, A1 = −0.06 ± 0.01, A2 = 1.02 ± 0.01; R214Q-Q2 + MiRP2, $V_{1/2}$ = −12.1 ± 1.3 mV, k = 18.4 ± 1.0 mV, A1 = −0.04 ± 0.01, A2 = 1.0 ± 0.01. (D) Top, exemplar current traces recorded in oocytes injected with wild-type (wt) KCNQ4 (Q4), R216H-KCNQ4, or double mutant R216H, R220Q-KCNQ4 (2R Q4) alone (top) or with MiRP2 (bottom) as indicated. Bars: (top traces) vertical, 1 μA; horizontal, 1 s; (bottom traces) vertical, 0.5 μA; horizontal, 1 s. Zero current level indicated by dashed lines. Bottom panels, mean I/V relationships for oocytes as above; n = 8–11. Error bars indicate SEM. (E) Mean G/V relationships for oocytes injected as in D, symbols as in D; n = 8–11. Error bars indicate SEM. Data were fitted with the Boltzmann equation; values were as follows: wild-type Q4, $V_{1/2}$ = −10.6 ± 1.6 mV, k = 18.3 ± 1.5 mV, A1 = 0.06 ± 0.02, A2 = 1.05 ± 0.02; wild-type Q4 + MiRP2, $V_{1/2}$ = −25.9 ± 2.1 mV, k = 15.4 ± 1.8 mV, A1 = 0.03 ± 0.02, A2 = 0.99 ± 0.03; R216H-Q4, $V_{1/2}$ = 33.8 ± 10.3 mV, k = 40.3 ± 4.5 mV, A1 = 0.0 ± 0.01, A2 = 1.5 ± 0.2; R216H-Q4 + MiRP2, $V_{1/2}$ = −11.6 ± 4.2 mV, k = 19.0 ± 3.6 mV, A1 = 0.19 ± 0.02, A2 = 1.06 ± 0.1; 2R Q4, $V_{1/2}$ = 16.1 ± 2.5 mV, k = 28.9 ± 2.0 mV, A1 = 0.15 ± 0.01, A2 = 1.19 ± 0.04; 2R Q4 + MiRP2, $V_{1/2}$ = −52.1 ± 14.3 mV, k = 12.5 ± 11.9 mV, A1 = 0.73 ± 0.1, A2 = 0.98 ± 0.02.

R220Q-KCNQ4 channels, we could compare the other set (Q244R-KCNQ1 with R216H-KCNQ4). Homomeric Q244R-KCNQ1 channels showed 40% of maximal tail current after a −120-mV prepulse, which was increased to 70% by MiRP2. Homomeric R216H-KCNQ4 channels showed essentially no tail current after a −120-mV prepulse, which was increased to 20% of maximal by MiRP2. These quantitative differences probably indicate that factors other than charge contribute to effects of mutagenesis in this region of S4, for example

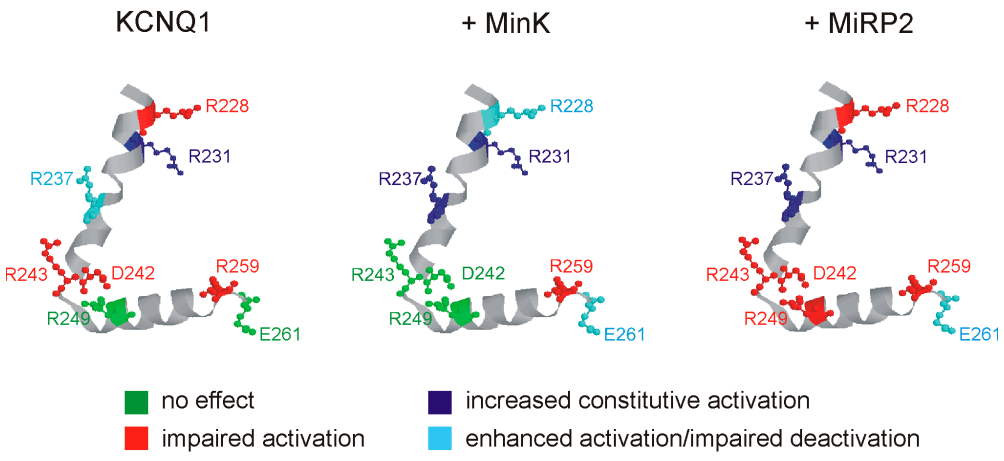

Figure 11. Summary of effects of charge perturbation in KCNQ1 S4. The KCNQ1 S4 and S4–S5 linker domains modeled on the Kv1.2 three-dimensional structure using SWISS-MODEL. The charged amino acids studied within are labeled and color coded according to their effects on the amount of constitutive current in KCNQ1 (left), MinK-KCNQ1 (center), and MiRP2-KCNQ1 (right) channels. Positions are color coded depending upon the relative activation properties of the less positively charged of the two variants tested at each position (alanine when basic residues were mutated, or the native residue when acidic residues were mutated). Thus, green indicates positions at which the less positively charged variant had no effect on activation; red indicates impaired activation; dark blue indicates increased constitutive activation; light blue indicates other enhancements of activation (left shifted voltage dependence) or slowed deactivation.

differences in local environment due to sequence differences in other nearby α subunit domains. However, in complexes with MiRP2, both Q244R-KCNQ1 and R216H-KCNQ4 showed levels of constitutive activation greater than that of the mutants in their homomeric form, and less than that of wild-type MiRP2-KCNQ1 channels. Further, mutation of the pair of residues (H240 and Q244 in KCNQ1; R216 and R220 in KCNQ4) was sufficient to swap activation properties of either α subunit in complexes with MiRP2. Overall, the data in Figs. 9 and 10 are consistent with the requirement for a lack of positive charge at positions 240 and 244 (KCNQ1 numbering) in conferring propensity for constitutive activation in MiRP2-KCNQ channels. The results strongly suggest that the KCNQ1 S4 charge balance, and specifically the paucity of positive charge in the CO_2H end of S4, is a primary determinant of conversion to leak by MiRP2.

DISCUSSION

We demonstrate that KCNQ1 has a unique S4 charge paucity in the CO_2H half, which in turn renders it susceptible to constitutive activation (leak), either by removal of a further single specific S4 charge at the NH_2 end, or by interaction with ancillary subunits. Potassium-selective leak channels provide a constant drive of the membrane potential toward the potassium equilibrium potential (E_K), in contrast to voltage-gated potassium channels that open in response to membrane depolarization and close upon repolarization to provide a dynamic mechanism for ending the action potential in excitable cells. KCNQ1 α subunits serve a variety of contrasting functions in different mammalian tissues, reliant upon profound shifts in functional properties endowed by MinK and related peptides. MinK-KCNQ1 channels generate the voltage-gated I_{Ks} repolarization current in human ventricular myocytes and the inner ear (Barhanin et al., 1996; Sanguinetti et al., 1996; Warth and Barhanin, 2002); inherited mutations in either MinK or KCNQ1 cause lethal cardiac arrhythmias and/or deafness (Splawski et al., 1997a,b; Tyson et al., 1997). MiRP2-KCNQ1 potassium channels form in the colon and are thought to regulate cAMP-mediated chloride secretion, a possible therapeutic target in secretory diarrhea and cholera (Schroeder et al., 2000b). MiRP1-KCNQ1 potassium channels facilitate gastric acid secretion from parietal cells into the stomach lumen by providing a K^+ ion efflux to balance K^+ influx through the H^+/K^+ ATPase, providing a possible therapeutic avenue for treatment of gastric ulcers (Tinel et al., 2000a; Grahammer et al., 2001; Heitzmann et al., 2004; Roepke et al., 2006).

Previous studies showed that MiRP2 transmembrane residue V72 is required for constitutive activation via interaction with S338 in the KCNQ1 S6 domain, placing MiRP2 close to the KCNQ1 channel pore (Melman et al., 2002, 2004; Panaghie et al., 2006). Furthermore, swapping of this central residue of the "activation triplet" within the transmembrane domain between MinK and MiRP2 bestows the activation properties of either subunit on complexes formed with KCNQ1; T58V-MinK/KCNQ1 complexes exhibit a degree of constitutive activation, whereas V72T-MiRP2-KCNQ1 complexes produce slowly activating currents (Melman et al., 2002). These data do not, however, explain why other voltage-gated potassium channels are not similarly affected by coassembly with MiRP2. KCNQ4 also bears a serine at a position equivalent to KCNQ1-S338 in the S6 (Kubisch et al., 1999) but is inhibited by MiRP2 (Schroeder et al., 2000b). Significantly, the activation of Kv3.1 and Kv3.2 is slowed by both MinK and MiRP2 with minimal changes in voltage dependence (Lewis et al., 2004), suggesting

that the contrasting effects of MinK and MiRP2 are relatively specific to KCNQ1. Further, the voltage dependence of Kv3.4 activation is negatively shifted by MiRP2 but without adoption of constitutive current (Abbott et al., 2001). MinK was previously shown, like MiRP2, to interact with KCNQ1 S6 (Melman et al., 2004; Panaghie et al., 2006) and here we show that MinK, like MiRP2, can form leak channels with KCNQ1 bearing single S4 domain point mutations, without mutagenesis of S6. We also demonstrate that S4–S5 linker charge integrity is required for normal function of MiRP2-KCNQ1 leak channels, either for communicating S4 position to the activation gate or for directly mediating other functional effects of MiRP2 on KCNQ1 activation.

The results of charge neutralization analyses in homomeric and heteromeric KCNQ1 channels are summarized in Fig. 11, which shows the KCNQ1 S4 and S4–S5 linker modeled on the structure of equivalent domains of the Kv1.2 channel (Long et al., 2005) with positions color coded depending upon the effects of mutagenesis on activation. Strikingly, both MinK-KCNQ1 channels and MiRP2-KCNQ1 channels showed increased constitutive current with the same basic residue mutations, in the N-terminal end of S4, that either caused constitutive activation (R231A) or greatly slowed the deactivation (R237A) of homomeric KCNQ1 channels. These data suggest that S4 position is similarly crucial in each channel type in determining the status of the activation gate, open or closed; a hypothesis further supported by the overall sensitivity of MiRP2-KCNQ1 activation to charge neutralizations throughout S4, most of which reduce constitutive activation. The finding that the charge status of a specific pair of residues in the CO_2H end of S4 (positions 240 and 244 in KCNQ1) determines whether MiRP2 can confer constitutive activation on KCNQ1 and KCNQ4 further supports the hypothesis that S4 is an active participant in wild-type MiRP2-KCNQ1 channels. Overall, the data suggest that stabilization of the KCNQ1 open state (or destabilization of the closed state) by MiRP2 across the physiological voltage range requires the exceptional S4 charge paucity observed in KCNQ1. Our data do not elucidate whether this is because KCNQ1 S4 bears insufficient charge to counteract interactions between MiRP2 and the activation gate that directly stabilize the open state or, alternatively, that MiRP2 stabilizes the open state by direct interaction with S4. It should be noted, however, that thus far there exists evidence for direct interaction of MiRP2 and MinK with KCNQ1 S6 but none for MiRP2 or MinK with KCNQ1 S4 (Melman et al., 2004; Panaghie et al., 2006).

For the sequence alignments in this study we used the "traditional" designation of S4, which corresponds to seven basic residues in *Shaker*, positioned at every third residue with two noncharged residues at either end (Aggarwal and MacKinnon, 1996). More recently, S4 has been delineated as a shorter domain, with the final CO_2H-end lysine being assigned to the S4–S5 linker, for example in the Kv1.2 crystal structure (Long et al., 2005). Either way, KCNQ1 S4 is unique among eukaryotic voltage-gated cation channels in its overall net charge paucity, and specifically in its CO_2H half electroneutrality, due to the presence of a single arginine (R243) with a neighboring aspartic acid (D242). A prokaryotic Kv channel, KvLm from *Listeria monocytogenes*, was recently cloned and found to contain a so-called "minimal" S4 domain, bearing only two of the four NH_2-end basic residues present in *Shaker*, and a single lysine in the +7 position from *Shaker* S4 (now often designated as S4–S5 linker as explained above) (Santos et al., 2006). In the more traditional designation, KvLm S4 has the same net charge as KCNQ1 S4, but markedly different properties; the $V_{1/2}$ of activation of KvLm is +154 mV (seemingly far from anything experienced in vivo) compared with −36 mV for homomeric KCNQ1 (Table I). It appears that the main principles of S4 charge and voltage gating are all-encompassing, but a myriad of different evolutionary solutions to distinct physiological problems has arisen, facilitated by the functional flexibility of S4 depending upon its net charge, the position of these charges, and the immediate environment created by juxtaposed channel domains.

In summary, our study provides the first comparison of the relative influence of specific S4 charges in the context of heteromeric potassium channels containing α and MiRP subunits. While both MinK and MiRP2 interact directly with the KCNQ1 pore (Melman et al., 2002, 2004; Panaghie et al., 2006), our results suggest that KCNQ1 S4 is a critical determinant of the relative effects of MinK and MiRP2, and that in complexes with MiRP2, KCNQ1 S4 adopts a conformation that favors the open state regardless of membrane potential. Because the exceptional charge paucity in the CO_2H half of wild-type KCNQ1 S4 is required for formation of constitutively active MiRP2-KCNQ channels, demonstrated by the S4 charge addition (to KCNQ1) and deletion (from KCNQ4) experiments, the results also identify for the first time α subunit–specific sequence determinants that dictate the α subunit–specific functional effects of MiRPs. Thus, KCNQ1 S4 charge paucity represents a unique specialization among eukaryotic voltage-gated cation channels, permitting KCNQ1 to act either as a constitutively open pore or a voltage-dependent channel in contexts dictated by overlapping expression of specific ancillary subunits, facilitating multiple prominent and diverse roles in mammalian physiology.

We are grateful to Aventis Pharmaceuticals for providing HMR1556.

G.W. Abbott is supported by the National Institutes of Health (R01 HL079275; RO3 DC07060).

Olaf S. Andersen served as editor.

Submitted: 28 June 2006
Accepted: 21 December 2006

REFERENCES

Abbott, G.W., M.H. Butler, S. Bendahhou, M.C. Dalakas, L.J. Ptacek, and S.A. Goldstein. 2001. MiRP2 forms potassium channels in skeletal muscle with Kv3.4 and is associated with periodic paralysis. *Cell.* 104:217–231.

Abbott, G.W., F. Sesti, I. Splawski, M.E. Buck, M.H. Lehmann, K.W. Timothy, M.T. Keating, and S.A. Goldstein. 1999. MiRP1 forms IKr potassium channels with HERG and is associated with cardiac arrhythmia. *Cell.* 97:175–187.

Aggarwal, S.K., and R. MacKinnon. 1996. Contribution of the S4 segment to gating charge in the Shaker K^+ channel. *Neuron.* 16:1169–1177.

Barhanin, J., F. Lesage, E. Guillemare, M. Fink, M. Lazdunski, and G. Romey. 1996. K(V)LQT1 and lsK (minK) proteins associate to form the I(Ks) cardiac potassium current. *Nature.* 384:78–80.

Grahammer, F., A.W. Herling, H.J. Lang, A. Schmitt-Graff, O.H. Wittekindt, R. Nitschke, M. Bleich, J. Barhanin, and R. Warth. 2001. The cardiac K^+ channel KCNQ1 is essential for gastric acid secretion. *Gastroenterology.* 120:1363–1371.

Heitzmann, D., F. Grahammer, T. von Hahn, A. Schmitt-Graff, E. Romeo, R. Nitschke, U. Gerlach, H.J. Lang, F. Verrey, J. Barhanin, and R. Warth. 2004. Heteromeric KCNE2/KCNQ1 potassium channels in the luminal membrane of gastric parietal cells. *J. Physiol.* 561:547–557.

Jensen, H.S., K. Callo, T. Jespersen, B.S. Jensen, and S.P. Olesen. 2005. The KCNQ5 potassium channel from mouse: a broadly expressed M-current like potassium channel modulated by zinc, pH, and volume changes. *Brain Res. Mol. Brain Res.* 139:52–62.

Jentsch, T.J. 2000. Neuronal KCNQ potassium channels: physiology and role in disease. *Nat. Rev. Neurosci.* 1:21–30.

Jiang, Y., V. Ruta, J. Chen, A. Lee, and R. MacKinnon. 2003. The principle of gating charge movement in a voltage-dependent K^+ channel. *Nature.* 423:42–48.

Kubisch, C., B.C. Schroeder, T. Friedrich, B. Lutjohann, A. El-Amraoui, S. Marlin, C. Petit, and T.J. Jentsch. 1999. KCNQ4, a novel potassium channel expressed in sensory outer hair cells, is mutated in dominant deafness. *Cell.* 96:437–446.

Lerche, C., G. Seebohm, C.I. Wagner, C.R. Scherer, L. Dehmelt, I. Abitbol, U. Gerlach, J. Brendel, B. Attali, and A.E. Busch. 2000. Molecular impact of MinK on the enantiospecific block of I(Ks) by chromanols. *Br. J. Pharmacol.* 131:1503–1506.

Lewis, A., Z.A. McCrossan, and G.W. Abbott. 2004. MinK, MiRP1 and MiRP2 diversify Kv3.1 and Kv3.2 potassium channel gating. *J. Biol. Chem.* 279:7884–7892.

Long, S.B., E.B. Campbell, and R. Mackinnon. 2005. Crystal structure of a mammalian voltage-dependent Shaker family K^+ channel. *Science.* 309:897–903.

McCrossan, Z.A., and G.W. Abbott. 2004. The MinK-related peptides. *Neuropharmacology.* 47:787–821.

Melman, Y.F., A. Krumerman, and T.V. McDonald. 2002. A single transmembrane site in the KCNE-encoded proteins controls the specificity of KvLQT1 channel gating. *J. Biol. Chem.* 277:25187–25194.

Melman, Y.F., S.Y. Um, A. Krumerman, A. Kagan, and T.V. McDonald. 2004. KCNE1 binds to the KCNQ1 pore to regulate potassium channel activity. *Neuron.* 42:927–937.

Panaghie, G., K.K. Tai, and G.W. Abbott. 2006. Interaction of KCNE subunits with the KCNQ1 K^+ channel pore. *J. Physiol.* 570: 455–467.

Piper, D.R., W.A. Hinz, C.K. Tallurri, M.C. Sanguinetti, and M. Tristani-Firouzi. 2005. Regional specificity of human ether-a'-go-go-related gene channel activation and inactivation gating. *J. Biol. Chem.* 280:7206–7217.

Roepke, T.K., A. Anantharam, P. Kirchhoff, S.M. Busque, J.B. Young, J.P. Geibel, D.J. Lerner, and G.W. Abbott. 2006. The KCNE2 potassium channel ancillary subunit is essential for gastric acid secretion. *J. Biol. Chem.* 281:23740–23747.

Sanguinetti, M.C., M.E. Curran, A. Zou, J. Shen, P.S. Spector, D.L. Atkinson, and M.T. Keating. 1996. Coassembly of K(V)LQT1 and minK (IsK) proteins to form cardiac I(Ks) potassium channel. *Nature.* 384:80–83.

Santos, J.S., A. Lundby, C. Zazueta, and M. Montal. 2006. Molecular template for a voltage sensor in a novel K^+ channel. I. Identification and functional characterization of KvLm, a voltage-gated K^+ channel from *Listeria monocytogenes*. *J. Gen. Physiol.* 128:283–292.

Schroeder, B.C., M. Hechenberger, F. Weinreich, C. Kubisch, and T.J. Jentsch. 2000a. KCNQ5, a novel potassium channel broadly expressed in brain, mediates M-type currents. *J. Biol. Chem.* 275:24089–24095.

Schroeder, B.C., S. Waldegger, S. Fehr, M. Bleich, R. Warth, R. Greger, and T.J. Jentsch. 2000b. A constitutively open potassium channel formed by KCNQ1 and KCNE3. *Nature.* 403:196–199.

Schwede, T., J. Kopp, N. Guex, and M. Peitsch. 2003. SWISS-MODEL: an automated protein homology-modeling server. *Nucleic Acids Res.* 31:3381–3385.

Sesti, F., and S.A. Goldstein. 1998. Single-channel characteristics of wild-type IKs channels and channels formed with two minK mutants that cause long QT syndrome. *J. Gen. Physiol.* 112:651–663.

Splawski, I., K.W. Timothy, G.M. Vincent, D.L. Atkinson, and M.T. Keating. 1997a. Molecular basis of the long-QT syndrome associated with deafness. *N. Engl. J. Med.* 336:1562–1567.

Splawski, I., M. Tristani-Firouzi, M.H. Lehmann, M.C. Sanguinetti, and M.T. Keating. 1997b. Mutations in the hminK gene cause long QT syndrome and suppress IKs function. *Nat. Genet.* 17: 338–340.

Starace, D.M., and F. Bezanilla. 2004. A proton pore in a potassium channel voltage sensor reveals a focused electric field. *Nature.* 427:548–553.

Takumi, T., H. Ohkubo, and S. Nakanishi. 1988. Cloning of a membrane protein that induces a slow voltage-gated potassium current. *Science.* 242:1042–1045.

Tinel, N., S. Diochot, M. Borsotto, M. Lazdunski, and J. Barhanin. 2000a. KCNE2 confers background current characteristics to the cardiac KCNQ1 potassium channel. *EMBO J.* 19:6326–6330.

Tinel, N., S. Diochot, I. Lauritzen, J. Barhanin, M. Lazdunski, and M. Borsotto. 2000b. M-type KCNQ2-KCNQ3 potassium channels are modulated by the KCNE2 subunit. *FEBS Lett.* 480: 137–141.

Tyson, J., L. Tranebjaerg, S. Bellman, C. Wren, J.F. Taylor, J. Bathen, B. Aslaksen, S.J. Sorland, O. Lund, S. Malcolm, et al. 1997. IsK and KvLQT1: mutation in either of the two subunits of the slow component of the delayed rectifier potassium channel can cause Jervell and Lange-Nielsen syndrome. *Hum. Mol. Genet.* 6:2179–2185.

Wang, H.S., Z. Pan, W. Shi, B.S. Brown, R.S. Wymore, I.S. Cohen, J.E. Dixon, and D. McKinnon. 1998. KCNQ2 and KCNQ3 potassium channel subunits: molecular correlates of the M-channel. *Science.* 282:1890–1893.

Warth, R., and J. Barhanin. 2002. The multifaceted phenotype of the knockout mouse for the KCNE1 potassium channel gene. *Am. J. Physiol. Regul. Integr. Comp. Physiol.* 282:R639–R648.

Yu, H., J. Wu, I. Potapova, R.T. Wymore, B. Holmes, J. Zuckerman, Z. Pan, H. Wang, W. Shi, R.B. Robinson, et al. 2001. MinK-related peptide 1: a β subunit for the HCN ion channel subunit family enhances expression and speeds activation. *Circ. Res.* 88: E84–E87.

Zhang, M., M. Jiang, and G.N. Tseng. 2001. minK-related peptide 1 associates with Kv4.2 and modulates its gating function: potential role as β subunit of cardiac transient outward channel? *Circ. Res.* 88:1012–1019.